HHS Public Access

Author manuscript

Mol Cancer Res. Author manuscript; available in PMC 2024 January 05.

Published in final edited form as:

Mol Cancer Res. 2023 July 05; 21(7): 675–690. doi:10.1158/1541-7786.MCR-22-0843.

Non-essential amino acid availability influences proteostasis and breast cancer cell survival during proteotoxic stress

Sara Sannino[1,*], **Allison M. Manuel**[2,4], **Chaowei Shang**[1], **Stacy G. Wendell**[2,3], **Peter Wipf**[5], **Jeffrey L Brodsky**[1,*]

[1]Department of Biological Sciences, University of Pittsburgh, Pittsburgh, PA, USA

[2]Health Sciences Mass Spectrometry Core, University of Pittsburgh, Pittsburgh, PA, USA

[3]Department of Pharmacology and Chemical Biology University of Pittsburgh, Pittsburgh, PA, USA

[4]Mass Spectrometry and Proteomics Core, The University of Utah, Salt Lake City, UT, USA

[5]Department of Chemistry, University of Pittsburgh, Pittsburgh, PA, USA

Abstract

Protein homeostasis (proteostasis) regulates tumor growth and proliferation when cells are exposed to proteotoxic stress, such as during treatment with certain chemotherapeutics. Consequently, cancer cells depend to a greater extent on stress signaling, and require the integrated stress response (ISR), amino acid metabolism, and efficient protein folding and degradation pathways to survive. To define how these interconnected pathways are wired when cancer cells are challenged with proteotoxic stress, we investigated how amino acid abundance influences cell survival when Hsp70, a master proteostasis regulator, is inhibited. We previously demonstrated that cancer cells exposed to a specific Hsp70 inhibitor induce the ISR via the action of two sensors, GCN2 and PERK, in stress-resistant and sensitive cells, respectively. In resistant cells, the induction of GCN2 and autophagy supported resistant cell survival, yet the mechanism by which these events were induced remained unclear. We now report that amino acid availability reconfigures the proteostasis network. Amino acid supplementation, and in particular arginine addition, triggered cancer cell death by blocking autophagy. Consistent with the importance of amino acid availability, which when limited activates GCN2, resistant cancer cells succumbed when challenged with a potentiator for another amino acid sensor, mTORC1, in conjunction with Hsp70 inhibition.

Implications: These data position amino acid abundance, GCN2, mTORC1, and autophagy as integrated therapeutic targets whose coordinated modulation regulates the survival of proteotoxic-resistant breast cancer cells.

[*]For correspondence: Sara Sannino, sannino.sara1986@gmail.com (SS); A321 Langley Hall, 4249 Fifth Avenue, Pittsburgh, PA 15260, +1412-624-4830; Jeffrey L. Brodsky, jbrodsky@pitt.edu (JLB), A320 Langley Hall, 4249 Fifth Avenue, Pittsburgh, PA 15260, +1412-624-4831.

The authors declare no potential conflicts of interest.

Introduction

Cancer cells can rewire metabolic pathways to meet their biosynthetic, redox, and energy requirements, and to maintain optimal levels of growth, proliferation, and metastasis. In many cases, stress response pathways play a critical role in these events. For example, the integrated stress response (ISR) rapidly induces the expression of adaptative proteins to optimize protein homeostasis (proteostasis), which is vital for cancer cell survival (1, 2). The ISR is mediated by downstream kinases, PERK (PKR-like endoplasmic reticulum resident kinase), GCN2 (general control non-derepressible 2), PKR (protein kinase RNA-activated) and/or HRI (heme-regulated inhibitor kinase) (3). These ISR kinases initially favor the accumulation of p-eIF2α (phosphorylated eukaryotic initiation factor 2 alpha), which blocks translation while concomitantly favoring the expression of transcription factors like ATF4 (activating transcription factor 4) (4, 5). In turn, ATF4 increases the expression of factors favoring angiogenesis, redox homeostasis, protein folding and degradation, and amino acid metabolism. Each of these proteostasis-supporting outcomes supports cancer initiation, survival, and resistance to stress and chemotherapy (6, 7). However, if proteotoxic stress is unmitigated, ISR activation instead induces the death of cancer cells by activating pro-apoptotic factors, such as CHOP (C/EBP homologous protein) (8). Efforts to use the ISR to kill cancer cells are in their early stages (9-11), and the roles of each ISR sensor in preserving cancer cell proteostasis are still unclear. Thus, a deeper understanding of the mechanisms involved in tumor cell resistance via ISR induction is needed to facilitate the development of combinatorial treatments.

Among the proteostasis pathways that support cancer cell survival are those that regulate protein degradation, i.e., autophagy and the ubiquitin-proteasome system (UPS), which destroy toxic aggregation-prone proteins (12, 13). Autophagy is directly enhanced by the ISR and influences tumor development, progression, and survival by regulating metabolism as well as organelle and protein quality control (11, 14-16). Thus, autophagy has also emerged as a target for anti-cancer therapies in established tumors (17-19).

Macromolecular precursors, such as amino acids and carbohydrates, fuel metabolic pathways and boost cancer cell survival, growth, and invasion (15, 20). Amino acids and amino acid metabolites are byproducts of the autophagy pathway and regulated by the ISR, respectively (16, 21). Moreover, many cancer cells are auxotrophic for specific amino acids, which are essential to synthesize new proteins and nucleosides and provide the raw material to generate ATP (22, 23). In addition to the ISR, the mammalian target of rapamycin complex 1 (mTORC1) also senses nutrient abundance in cancer cells (24). In brief, increased accumulation of specific amino acids activates mTORC1, favoring mRNA translation and lipid/nucleotide biosynthesis. In contrast, mTORC1 inhibition favors catabolic pathway induction, e.g. autophagy (25, 26). Not surprisingly, the ISR and mTORC1 are interconnected; GCN2-ATF4 induction sustains mTORC1 inhibition in cancer models (7, 27).

Another link between cancer and each of the proteostasis pathways outlined above is provided by molecular chaperones, which directly support protein biogenesis, degradation, and transport (28). ISR induction increases the expression of chaperones, such as heat

shock protein 70 (Hsp70), which are required for cancer cell survival when challenged with proteotoxic stress (29, 30). In fact, Hsp70 inhibition sensitizes some cancers to secondary chemotherapeutic treatments (31-33), and we recently demonstrated that rhabdomyosarcomas and breast cancer cells exposed to a site-specific allosteric Hsp70 inhibitor, MAL3-101 (34, 35), exhibit signs of proteostasis collapse, which favors ISR pathway induction (11, 36, 37). Interestingly, breast cancer cells binned into two groups, i.e., MAL3-101 sensitive and resistant. Inhibitor-*sensitive* breast cancer cells treated with MAL3-101 accumulate p-eIF2α and CHOP, suggesting that the ISR, and in particular PERK, initiate apoptosis (11, 36, 37). However, inhibitor-*resistant* breast cancers succumb to MAL3-101 when GCN2 is silenced, indicating that GCN2 is required for their survival (11). Yet, the resistant cells could now be killed when treated with both MAL3-101 and a clinical autophagy inhibitor. These data suggested that amino acids—derived from autophagy—modulate the survival of resistant breast cancer cells, and that ISR/GCN2 activation as well as mTORC1 inhibition also favor survival.

We now show that Hsp70 inhibition directs ISR signaling by mimicking amino acid depletion, thus activating both the PERK and GCN2 legs of the ISR. This in turn favors autophagy and resistant breast cancer cell survival. We also show that inducing both PERK and mTORC1 inhibits autophagy and—especially in the presence of the Hsp70 inhibitor—initiates the death of resistant breast cancer cells. However, cancer cell apoptosis was alleviated by amino acid starvation and upon PERK and/or mTORC1 inhibition. Furthermore, arginine supplementation impaired autophagy, activated mTORC1, and induced cancer cell death. We conclude that—to maintain proteostasis—resistant breast cancer cells must coordinate the functions of ISR, mTORC1, autophagy, and amino acid metabolism to survive, and that novel combinatorial treatments targeting these pathways may yield effective outcomes in proteotoxic- and chemotherapy-resistant breast cancers.

Materials and Methods

A detailed description of reagents, antibodies, and their sources can be found in the Supplementary Materials and Methods Supplementary Table 1.

Cell lines

MDA MB 453 (RRID:CVCL_0418), MDA MB 468 (RRID:CVCL_0419), and MDA MB 231 (RRID:CVCL_0062) lines were purchased from ATCC, and HCC38 (RRID:CVCL_1267) cells were obtained as previously described (11). All cell lines were grown at 37°C in 5% CO_2 in RPMI-1640 media supplemented with 10% FBS (fetal bovine serum) and 1x penicillin/streptomycin (PenStrep). Cells were shown to be *Mycoplasma*-free via diagnostic PCR (ATCC Mycoplasma detection kit), as per the manufacturer's instructions. All the lines were authenticated using the University of Arizona Genetics Core (Tucson, Arizona) by short tandem repeat DNA Profiling. RFP-GFP-LC3B-expressing MDA MB 231 and MDA MB 453 clone generation was previously described (11). Clonal lines were grown in RPMI-1640 media supplemented with 10% FBS with G418 at a final concentration of 350 μg/mL (Geneticin). Upon clonal line generation, the cells were again

shown to be *Mycoplasma*-free. Only early passage cells (p1 and p2) after thawing were used.

Cell culture and treatments

RFP-GFP-LC3 stably expressing MDA MB 231 and MDA MB 453 cells were seeded at 220,000 cells/well in 6-well plates and allowed to adhere overnight before treatment. MAL3-101 (38) and everolimus were dissolved in DMSO (dimethyl sulfoxide) to a final concentration of 20 mM, while NV-5138 was prepared at a final concentration of 5 mM. GSK-2606414 was dissolved to a final concentration of 50 mM in DMSO. MAL3-101 and everolimus were stored at −20°C, and NV-5138 aliquots were kept at −80°C. L-arginine monohydrochloride and L-lysine monohydrochloride were dissolved in sterile D-PBS (phosphate buffered saline) to a final concentration of 200 mM. Prior to use, the desired amount of each compound, including amino acids, was added to pre-warmed media, mixed thoroughly, and added onto cells.

To inhibit mTORC1, cells were treated with 3 μM everolimus for 6 h in the presence of 20 μM MAL3-101 or an equivalent volume of the vehicle. To assay mTORC1 activation, cells were exposed to DMSO or 20 μM MAL3-101 for 6 h. Two hours before the end of the 6 h time point, 10 μM NV-5138 or a corresponding volume of DMSO was added for 2 h. Everolimus and NV-5138 concentrations were selected after dose titration (1, 2, 3, 5, 10 μM) and monitoring p-p70S6K (mTORC1 activation) (24), cleaved caspase-8 (apoptosis) (39), and Hsp70 abundance (cell stress) (31) by immunoblot. To investigate the effects of amino acids, cells were washed twice in sterile D-PBS before incubation in amino acid deficient RPMI media supplemented with 10% dialyzed FBS and 17.6 mM D-(+)-glucose for 1 h. After 1 h of amino acid starvation, cells were then incubated in the same media (-AA) or in media supplemented with non-essential amino acids (NEAA) and 100 μM arginine and lysine (+NEAA), 100 μM arginine alone (+Arg), or only 100 μM lysine (+Lys) for 5 h in the presence or absence (DMSO) of 20 μM MAL3-101. In some cases, cells were instead exposed to regular RPMI with 10% dialyzed FBS in the presence or absence of MAL3-101 (Complete). To define the role of PERK activation when amino acid availability was altered, cells were treated with 4 μM GSK-2606414 for 5 h (1 h after amino acid starvation) in the presence or absence (DMSO) of 20 μM MAL3-101.

Immunoblot analysis

Cells were plated and treated as above and samples were collected, lysed, and processed for immunoblotting (11). Antibodies are listed in Supplementary Table 1. In all cases, proteins were visualized using a 1:1 mix of ProSignal® Pico and ProSignal® Femto ECL Reagent (Prometheus Laboratories Inc., California), and images were taken using a Bio-Rad ChemiDoc XRS+ with Image Lab software. Data were analyzed using ImageJ software (National Institutes of Health, RRID:SCR_003070).

Cell viability assays

Cells were plated in 96-well clear-bottomed plates (Greiner bio-one), and after 72 h of treatment, the CellTiter-Glo reagent was added and luminescence read on a Bio-Rad ChemiDoc XRS+ with the associated Image Lab software (Bio-Rad, Thermo Fisher

Scientific, RRID:SCR_014210). Under conditions in which media was supplemented with NEAA, 24 h after cell seeding, media was replaced with 10% dialyzed FBS containing RPMI media or amino acid-free RPMI supplemented with 100 μM NEAA, 100 μM arginine and lysine, 17.6 mM D-(+)-glucose and 10% dialyzed FBS (+NEAA). Cells were treated with MAL3-101 as described (11).

Analysis of cell surface Annexin-V was performed by staining cells with the Annexin-V Apoptosis Detection Kit following the manufacturer's instructions. After exposure to the indicated treatments, parental MDA MB 231 and MDA MB 453 cells were collected and stained as reported (11). Samples were analyzed on an Attune NxT Flow Cytometer (Thermo Fisher Scientific). Flowjo software was used for analysis (FlowJo™ v10 Software - BD Biosciences, San Diego, RRID:SCR_008520). Annexin-V and Annexin-V/PI (propidium iodine) double positive cells were summed and represented as the percentage of apoptotic cells.

Confocal microscopy

RFP-GFP-LC3B expressing cells were seeded at a density of 250,000 cells in 35 mm MatTek dishes (P35GC-1.5-10-C, MatTek Corporation). After 24 h, the cells were starved for amino acids for 1 h and then samples were treated with EBSS (Earle's balanced salt solution) and MAL3-101 (15 μM) or DMSO for 5 h. Cells were viewed live on a Nikon A1R point scanning confocal microscope with 5% CO_2 at 37 °C to measure autophagosome and autophagolysosome formation by monitoring RFP and GFP fluorescent signals. Data analysis was performed using Nikon's NIS-Elements software (Nikon Instrument, RRID:SCR_014329). 3D-threshold and bright spot detection tools identified and quantified the number of RFP and GFP positive puncta per cell after equalizing signal intensity using the LUTs - Non-destructive Image Enhancement tool (11). To obtain representative images, maximum intensity projections of 0.2 μm steps though the entire cell were generated using Nikon's NIS-Elements software. Scale bars = 50 μm.

Amino acid analysis

A total of 220,000 cells were seeded in 6-well plates with 10% normal FBS containing media and adhered overnight before treatment with vehicle or 5 μM MAL3-101 for 24 h. Targeted metabolomic studies were completed for control and MAL3-101 treated MDA-MB 231 and MDA-MB 453 cell lines via liquid chromatography-high resolution mass spectrometry (LC-HRMS) for free amino acids. Metabolic quenching and polar metabolite extraction were performed using 1 mL of ice-cold 80% methanol/0.1% formic acid after washing cells (1 X 10^6) with PBS. A stable isotope internal standard mix containing creatinine-d3, alanine-d3, taurine-d4 and lactate-d3 (Sigma-Aldrich) was added at a final concentration of 100 μM. After 3 min, the supernatant was cleared by centrifugation at 16,000 *g*. Cleared supernatant (3 μL) was injected via a Thermo Vanquish UHPLC and separated over a reversed-phase Thermo HyperCarb porous graphite column (2.1 × 100 mm, 3-μm particle size) maintained at 55 °C. For the 20 min LC gradient, the mobile phase consisted of the following: solvent A (water/0.1% formic acid) and solvent B (acetonitrile/0.1% formic acid). The gradient was: 0–1 min 1% B, increasing to 15% B over 5 min, increasing to 98% B over 5 min, and held at 98% B for 5 min before equilibration to

starting conditions. The Thermo ID-X tribrid mass spectrometer was operated in positive and negative ion mode, scanning in full MS mode (2μscans) from 100 to 800 m/z at 70,000 resolution with an automatic gain control target of 2×10^5. The source ionization setting was 3.0 kV spray voltage for positive mode. Source gas parameters were 45 sheath gas, 12 auxiliary gas at 320 °C, and 8 sweep gas. Calibration was performed before analysis using the Pierce FlexMix Ion Calibration Solution (Thermo Fisher Scientific). Alignment and peak area integration were then extracted manually using the Quan Browser (Xcalibur ver. 2.7; Thermo Fisher Scientific, RRID:SCR_014593). Data were reported as peak area ratio of the analyte to ISTD normalized to mg of protein. To obtain an estimate of amino acid abundance changes in control versus MAL3-101 treated cells, the mean fold change of the indicated amino acids is shown in Fig. 1A (n=4).

Statistical analysis

IC_{50} concentrations from CellTiter-Glo assays were calculated as described (37) using SigmaPlot 11.0 (Systat Software, Inc., RRID:SCR_003210). GraphPad Prism 9 (GraphPad Software, Inc., RRID:SCR_002798) was used for two-tailed Student's t tests between two samples, and a non-parametric Kruskal-Wallis test analysis was performed to establish statistical significance between multiple conditions compared to the control. In all experiments, significance was determined at ≤ 0.05.

Data availability statement

All data generated in this study are available within the article and its Supplementary files. Unique materials used in this study are available upon request from the corresponding authors.

Results

Non-essential amino acids regulate breast cancer cell viability during proteotoxic stress

Despite the encouraging efficacy of recently developed anticancer agents, many tumors fail to respond to traditional chemotherapy, target-therapy, and/or radiotherapy, or develop resistance (40, 41). To better define the mechanisms underlying breast cancer resistance to proteotoxic stress induced by chemotherapeutics (42), we previously investigated how cancer cells react to proteostasis collapse by inhibiting Hsp70 with a specific modulator, MAL3-101 (11). Breast cancer lines that were sensitive to the inhibitor underwent an ISR pathway-mediated apoptosis via PERK activation, accumulating both p-eIF2α and the pro-apoptotic protein CHOP. ISR or PERK inhibition also prevented cell death upon proteotoxic stress exposure. In stress-resistant cells, the ISR pathway was similarly activated, but CHOP accumulation was absent. Instead, another ISR sensor, GCN2, was activated, which induced autophagy (11). In addition, inhibiting GCN2 and/or autophagy in combination with the Hsp70 inhibitor could kill resistant breast cancer cells, but the mechanism(s) underlying GCN2, and autophagy induction were unclear.

Cancer cells modulate amino acid metabolic pathways to survive (23, 43), and previous work indicated that autophagy and GCN2 induction—as well as activation of the nutrient sensor, mTORC1—are amino acid regulated (16, 44-48). Consistent with these data, Hsp70

inhibitor sensitivity was reduced in the presence of an FDA-approved mTORC1 inhibitor, everolimus (11, 49). Since mTORC1 activation is stimulated by increased accumulation of select amino acids (50, 51) and, once activated, mTORC1 prevents autophagy (25, 52), we hypothesized that amino acids dictate the induction of compensatory pathways (i.e., autophagy) when cells are confronted with proteotoxic stressors, such as the Hsp70 inhibitor MAL3-101.

To test this hypothesis, we applied MAL3-101 and profiled free amino acid content in Hsp70 inhibitor sensitive (MDA MB 231) and resistant (MDA MB 453) triple negative breast cancer (TNBC) cells, an invasive breast cancer subtype with high tumor recurrence after treatment with proteotoxic chemotherapies (42, 53) (Fig. 1A). The levels of most measured free amino acids increased in stress-sensitive but not resistant cells. Notably, two non-essential amino acids (NEAAs), asparagine and arginine—which cancer cells can produce for protein/nucleotide synthesis and energy (43)—and an essential amino acid, lysine, rose most substantially (3.0, 4 and 3.3 fold higher, respectively) in stress-sensitive cells upon treatment. Arginine and lysine levels were comparable in DMSO treated stress-sensitive and resistant cells (arginine levels: 57±6 and 56±10; lysine levels: 5±0.5 and 5±0.8 in MDA MB 231 and MDA MB 453 cells, respectively), indicating that their change in sensitive cells was mediated by the proteotoxic stressor. Interestingly, arginine, which activates mTORC1 and inhibits autophagy (54, 55), showed the greatest increase. These results suggest that a proteostasis imbalance in sensitive cells leads to the accumulation of select free amino acids, which activate mTORC1, inhibit autophagy, and prevent the induction of this pro-survival pathway.

To test whether overall NEAA abundance influences TNBC sensitivity to proteotoxic stress, we measured MAL3-101 sensitivity in the presence or absence of media supplemented with NEAAs in sensitive and resistant cells. TNBC sensitive MDA MB 231 and MDA MB 468 and resistant MDA MB 453 and HCC38 cells, as well as clones of the parental MDA MB 231 and MDA MB 453 lines that stably express RFP GFP LC3B (which reports on autophagy; see below), were used. As shown in Fig. 1B, little effect was seen in stress-sensitive cells (MDA MB 231, MDA MB 468 and MDA MB 231 RFP GFP LC3B, indicated in blue), but NEAA supplementation more prominently increased MAL3-101 sensitivity in resistant lines (MDA MB 453, HCC38 and MDA MB 453 RFP GFP LC3B, indicated in black text) (Fig. 1C; IC50s of stress-resistant MDA MB 453, HCC38 and MDA MB 453 RFP GFP LC3B cells dropped from ≥ 30 μM to 6.3 μM, 10 μM and 5.9 μM, respectively). The introduction of the stable RFP-GFP-LC3B autophagy reporter (see below) had little effect on these responses, so all subsequent studies used these lines (hereafter called MDA MB 231 and MDA MB 453), unless indicated otherwise. These results indicate that NEAAs decrease the survival of resistant breast cancer cells when exposed to a proteotoxic stressor.

As expected, when cells were exposed to MAL3-101 in complete media, apoptosis was only evident in stress-sensitive cells, MDA MB 231, as seen by cleaved caspase-3 and caspase-8 and were not further sensitized when NEAAs were added (Fig. 1D-E). In contrast, apoptotic markers were absent in the MAL3-101-treated resistant MDA MB 453 cells, but cleaved caspase-3 and caspase-8 now accumulated when NEAAs were added with MAL3-101. These data confirm that NEAA addition induces breast cancer cell death when proteostasis

is compromised. Also in agreement with the data shown above, amino acid depletion (-AA) had no effect on resistant cell survival upon proteotoxic stress, but stress-sensitive cells exposed to MAL3-101 in media deprived of amino acids showed reduced accumulation of both cleaved caspase-3 and caspase-8 (Fig. 1D-E). These results show that amino acid abundance alters proteostasis, as reported (44, 56-58), but may also be harnessed to provide a potential therapeutic outcome when combined with a proteotoxic stressor, such as MAL3-101 or select chemotherapies, in resistant TNBCs.

Autophagy is inhibited by non-essential amino acids in resistant breast cancer cells

Autophagy destroys damaged proteins and organelles and recycles cytosolic components (18, 59, 60). There are three main forms of autophagy: macroautophagy (hereafter called autophagy), microautophagy, and chaperone-mediated autophagy (61). Autophagy is also utilized by healthy cells to safeguard proteostasis, but can be induced following stress (i.e., after chemotherapeutic treatments) to increase cancer cell survival (60, 61). Autophagy is characterized by substrate recruitment into a double-membrane vesicle, an autophagosome, that fuses with the lysosome to form autophagolysosomes in which contents are destroyed and recycled into amino acids and other building blocks that fuel metabolism (62). In line with the role of autophagy as a pro-survival pathway, we demonstrated that stress-resistant cells require autophagy to survive proteotoxic stress (11, 36).

To determine the effect of NEAAs on autophagy, we performed dual-color live imaging experiments in stress-sensitive and resistant cells, which stably express RFP GFP LC3 (63). In brief, RFP GFP LC3 decorates autophagosomes, which are detected as yellow vesicles (RFP^+GFP^+), but when yellow autophagosomes fuse with lysosomes, the lower pH quenches GFP, allowing the visualization of autophagolysosomes as red vesicles (RFP^+GFP^-) (Fig. 2A). Therefore, autophagy flux and delivery of autophagosomes to lysosomes is visualized as an increase in RFP^+GFP^- puncta versus RFP^+GFP^+ autophagosomes. In agreement with our previous work (11), RFP^+GFP^- puncta accumulated in stress-resistant (MDA MB 453) but not in stress-sensitive (MDA MB 231) cells when Hsp70 was inhibited in complete media, indicating that stress-resistant cells induce autophagy when exposed to proteotoxic stress, i.e., MAL3-101 (Fig. 2B-C and quantified in Fig. 4C-D). Interestingly, when NEAA and MAL3-101 were added together, RFP^+GFP^- puncta were reduced in resistant cells, indicating that these amino acids prevent induction of a survival pathway, autophagy, in stress-resistant cells (Fig. 2C and Fig. 4D, +NEAA). In contrast, autophagy flux was unaffected by NEAAs in sensitive cells (Fig. 2B and Fig. 4C), consistent with the idea that these amino acids are elevated upon MAL3-101 treatment (Fig. 1A). As a control, RFP^+GFP^- puncta in both stress-sensitive and resistant lines increased upon amino acid starvation, regardless of whether MAL3-101 was present (Fig. 2B-C and Fig. 4C-D, -AA).

Arginine is sufficient to kill breast cancer cells exposed to proteotoxic stress

The data in Fig. 1A indicated that arginine and lysine accumulate to the highest extent. To examine their contributions, we measured apoptotic marker accumulation in stress-sensitive and resistant cells exposed to MAL3-101 in media containing arginine or lysine (+Arg and +Lys, respectively; Fig. 3A). Minimal cleaved caspase 3 was present in amino acid

starvation media (-AA) in stress-sensitive (MDA MB 231) and stress-resistant (MDA MB 453) cells, regardless of whether MAL3-101 was present, and cleaved caspase 8 levels declined when MAL3-101 was added (-AA; Fig. 3A and quantified in Fig. 3C). These data are consistent with autophagy induction (Fig. 2) and stress protection. However, when arginine was added, cleaved caspase-3 and caspase-8 now accumulated in stress-sensitive and resistant cells exposed to MAL3-101. Yet, lysine had little effect. Thus, even though arginine and lysine accumulate, only arginine drives drug-dependent apoptosis induction in sensitive and resistant cells when amino acids are limiting.

To confirm these data, we monitored apoptosis induction via annexin-V and propidium iodine (PI) staining under conditions in which amino acid levels were altered in the presence or absence of MAL3-101 (Fig. 3B). In complete media, the percentage of apoptotic stress-sensitive cells (MDA MB 231) rose in the presence of MAL3-101, but Hsp70 inhibition had no effect on apoptosis in stress-resistant cells (MDA MB 453), consistent with our prior work and the results presented above (11). In contrast, MAL3-101-induced proteotoxic stress in amino acid depleted media prevented apoptosis in both lines, supporting the fact that amino acid starvation boosts autophagy and favors survival. Finally, although NEAA, arginine, or lysine had no effect in stress-sensitive and -resistant cells, NEAA or arginine addition to MAL3-101-containing media increased the percentage of stress-resistant apoptotic cells. These data establish that combining amino acid availability with a specific proteotoxic stress—such as via an Hsp70 inhibitor—kills stress-resistant breast cancer cells.

Since we reported that the ISR sensor PERK was induced in stress-sensitive and resistant cells exposed to MAL3-101 (11), we also monitored ISR induction under each condition (Fig. 3A). We first confirmed PERK activation by monitoring phosphorylation (p-PERK) via its migration after SDS-PAGE and immunoblotting. PERK mobility was reduced to a similar extent in stress-sensitive and -resistant cells when exposed to MAL3-101, suggesting comparable PERK activation in both lines and under all the media conditions. Likewise, the general ISR marker p-eIF2α accumulated in both stress-sensitive and resistant cells when Hsp70 activity was compromised (Fig. 3A and Fig.S1A). However, as previously reported (11), the pro-apoptotic protein CHOP was detected only in stress-sensitive MDA MB 231 cells when Hsp70 was inhibited in complete media. These data suggest that PERK is responsible for stress-dependent apoptosis in sensitive cells. In contrast, when arginine was added to MAL3-101 treated cells, p-eIF2a levels were unaffected but CHOP accumulated in both lines (Fig. 3A and Fig. S1 A-B). Yet, CHOP was absent when lysine was added to Hsp70-containing media, demonstrating the selective effect of arginine. Nevertheless, moderate CHOP accumulation was seen when stress-sensitive and resistant cells were exposed to MAL3-101 in amino acid depleted media, suggesting that CHOP, but not other apoptotic markers (i.e., cleaved caspase-3), respond to proteotoxic stress when amino acids are limiting (Fig. 3A-C and Fig. S1B). Interestingly, stress-induced ATF4-CHOP heterodimers were reported to act downstream of ISR to upregulate several autophagy-requiring genes after amino acids are deprived, with no effects on cell viability (16, 64, 65). Regardless, these results position NEAAs, and in particular arginine, as a trigger for breast cancer cell death via the ISR when proteostasis is compromised in resistant cells.

Arginine inhibits autophagy in stress-resistant cells exposed to a proteotoxic stressor

To address the mechanism by which arginine favors apoptosis in stressed breast cancer cells, we again monitored autophagy flux in sensitive and resistant cells under various conditions. We first confirmed that autophagy is induced only in stress-resistant (MDA MB 453) cells exposed to proteotoxic stress (Fig. 4A-B and Fig. 4C-D, compare DMSO and MAL3-101, Complete). However, arginine supplementation prevented the accumulation of $RFP^{+}GFP^{-}$ puncta, i.e., autophagy induction. On the contrary, no major alterations in MAL3-101-mediated autophagy flux were detected in stress-resistant cells exposed to proteotoxic stress in lysine supplemented media (Fig. 4B and Fig. 4D, compare +Arg and +Lys conditions). These results confirm that arginine prevents autophagy activation, thus ablating stress-resistant breast cancer cell survival when proteostasis collapses. On the contrary, autophagic flux continued in the resistant cells when lysine was supplemented into the media.

GCN2 and PERK have opposite roles in breast cancer survival when proteostasis is compromised

We showed that ISR induction can be cytoprotective or pro-apoptotic, depending on how the activation of different ISR legs (PERK and GCN2) is integrated when proteostasis is compromised (11). In Figure 3, we showed that PERK is induced in stress-sensitive and resistant cells exposed to proteotoxic stress, but amino acid addition had no effect on p-PERK or p-eIF2α accumulation in both lines (Fig. 3A). To further address the mechanism by which NEAAs and arginine favor apoptosis in the presence of proteotoxic stress, we treated stress-sensitive and resistant cells with the PERK inhibitor, GSK-2606414 (GSK) (66) and measured apoptosis when Hsp70 activity was impaired in complete media or in the presence of NEAAs (Fig. 5A). In line with our published data (11), GSK-2606414 reduced apoptosis in sensitive cells, even upon Hsp70 inhibition in complete media, whereas stress-resistant cell viability was unaltered when PERK activity was compromised (Fig. 5A, compare Complete and GSK). These data confirm the role of PERK as cytotoxic trigger when the proteostasis pathway is overwhelmed in complete media. Interestingly, while NEAA addition favors apoptosis in the presence of a stressor, GSK-2606414 in the presence of MAL3-101 in NEAA media reduced apoptosis in both stress-sensitive and resistant cells (Fig. 5A, compare NEAA and GSK+NEAA samples). Thus, amino acid supplementation favors PERK-mediated apoptosis when proteostasis is compromised in breast cancer cells. As a control, the efficacy of GSK-2606414 was validated since the higher molecular weight p-PERK signal was abolished in MAL3-101 treated cells (Fig. 5B).

Another ISR leg, exemplified by GCN2, activates MAL3-101-dependent autophagy, favoring cancer cell survival when Hsp70 is inhibited in complete media (11). To investigate the role of GCN2 in the presence of arginine, we first monitored the phosphorylation of Thr-899, which resides in the GCN2 activation-loop (p-GCN2), when sensitive and resistant cells were exposed to MAL3-101 in complete and arginine supplemented media (Fig. 5C). p-GCN2 accumulated to a higher extent in stress-resistant cells in complete media (Fig. 5C-D), suggesting that the MAL3-101 induced decline in amino acids activates GCN2 (along with autophagy) to favor survival. Interestingly, p-GCN2 accumulation was abolished when cells were exposed to MAL3-101 in the presence of arginine (Fig. 5C-D), suggesting

that amino acid supplementation (e.g., arginine) impairs GCN2 (but not PERK) activation in stress-resistant cells faced with proteotoxic stress. As expected, no major changes were detected in p-GCN2 accumulation in stress-sensitive cells when Hsp70 was inhibited in each condition (Fig. 5C-D). These data establish that arginine blocks GCN2 and autophagy activation, favoring breast cancer cell death in the presence of MAL3-101.

The ISR markers p-eIF2α and CHOP accumulated after MAL3-101 treatment in arginine supplemented media (Fig. 3A). To investigate the role of arginine in ISR induction in MAL3-101 treated stress-sensitive and resistant cells, ATF4 accumulation was monitored (Fig. 5C-E). ATF4 accumulated when Hsp70 was compromised in both cell types, confirming ISR activation (Fig. 5C-E). However, arginine supplementation had little effect on ATF4 in combination with MAL3-101, confirming the involvement of the ISR pathway, and specifically of PERK (see above), in triggering cancer cell death when proteostasis is compromised. Of note, a minor but not statistically significant accumulation of ATF4 was detected when arginine was added to the media of stress-resistant cells in the absence of any stress. This phenomenon might be ISR-independent but mTORC1-activation dependent, as reported in other cellular models (67).

As mentioned above, unmitigated ISR activation can be cytotoxic when cells are exposed to proteotoxic stress, and the activation of caspase 8 was previously linked to the ISR- and UPR- (unfolded protein response) mediated regulation of death markers, including CHOP and death receptor family members (DR) (68). It was also reported that ATF4 and CHOP are individually required to induce DR5 expression in the presence of proteotoxic stress (69-73). Therefore, DR5 accumulation was monitored when Hsp70 activity was impaired in complete and arginine supplemented media (Fig. 5C-F). Interestingly, there was some accumulation of DR5 detected when MAL3-101 was added to arginine supplemented media, suggesting that DR proteins might also be involved. However, since the same effect was not detected in stress-sensitive cells we cannot exclude the possibility that other DR proteins might contribute to this process, as seen in other systems (70-73). Nevertheless, our results confirm that arginine prevents GCN2 but not PERK activation, thus blunting stress-resistant breast cancer cell survival and favoring PERK-mediated cell apoptosis when proteostasis collapses.

mTORC1 activation supports cancer cell death when challenged with proteotoxic stress

Under amino acid-rich conditions, mTORC1 is activated at the lysosomal membrane (74) and increases the phosphorylation of downstream targets, such as the protein 70S6 kinase (p70S6K), to activate anabolic pathways and inhibit catabolic pathways, such as autophagy (Fig. 6A) (25, 75). Since arginine activates mTORC1 (50, 54), and knowing that arginine prevented autophagy and initiated the death of stress-resistant cancer cells (see above), we asked whether mTORC1 contributes to the apoptotic pathway in sensitive and resistant cells exposed to proteotoxic stress.

First, to evaluate the effect of MAL3-101 on mTORC1 signaling, we measured p-p70S6K accumulation in both cell lines in the presence or absence of MAL3-101. As shown in Fig. 6B-C-D, there were lower levels of p-p70S6K in stress-resistant cells exposed to proteotoxic

stress, while no statistically significant changes in p-p70S6K were detected between DMSO and MAL3-101 treated MDA MB 231 (stress-sensitive) cells (Fig. 6B-D).

Second, we asked if modulating mTORC1 activity altered the ISR and cancer cell apoptosis in stress-sensitive and-resistant cells in the presence of MAL3-101. To boost mTORC1 activation, we used NV-5138, a Sestrin-2 inhibitor that prevents Sestrin-GATOR2 complex formation and activates mTORC1 (76). Therefore, both lines were treated with NV-5138 over time in the presence or absence of MAL3-101. mTORC1 activation and cell death were then monitored in sensitive and resistant cells. Administration of NV-5138 alone increased p70S6K phosphorylation in both lines, and when NV-5138 was combined with MAL3-101, p-p70S6K accumulated to a higher extent, suggesting mTORC1 activation (Fig. 6B-C). Interestingly, after 2 h of NV-5138 treatment in the presence of MAL3-101, a drop in p-p70S6K levels was detected, which corresponded with cleaved caspase 8 accumulation (Fig. 6B-C). This phenomenon was more evident in stress-resistant cells and appeared to be linked to increased cell death, potentially reflecting altered protein synthesis and/or kinase signaling activation after proteostasis collapse. These results suggest that altered mTORC1 activation via NV-5138 favors breast cancer cell death when they are confronted with proteotoxic stress.

To better define the role of mTORC1 activation in breast cancer cells faced with a proteotoxic stressor, we next monitored ISR induction and cell apoptosis when stress-sensitive and resistant cells were treated with MAL3-101 in the presence or absence of NV-5138. As expected, NV-5138 administration increased p-p70S6K in vehicle-treated MDA MB 231 and MDA MB 453 lines (stress-sensitive and resistant cells, respectively). When NV-5138 was administered in combination with MAL3-101, no major effects were observed on p-eIF2α (Fig. 6D), yet NV51-38 treatment favored CHOP and cleaved caspase-3 and caspase-8 accumulation in resistant cells treated with MAL3-101 (Fig. 6D and Fig. S1C-D-E). However, apoptosis was unaltered in stress-sensitive cells regardless of whether NV-5138 was present. Overall, our results indicate that a MAL3-101-mediated proteostasis imbalance favors amino acid depletion, reduces mTORC1 activation, and boosts autophagy to help resistant cancer cells cope with stress.

Third, to confirm the role of mTORC1 during stress-sensitive and resistant cell death when proteostasis is impaired, we monitored apoptotic cells via annexin-V/PI staining in in the presence or absence of MAL3-101 and when mTORC1 activity was either inhibited or enhanced with everolimus or NV-5138, respectively. mTORC1 inhibition reduced the percentage of apoptotic cells when stress-sensitive cells were exposed to MAL3-101, while under identical conditions no change in the annexin-V/PI population of stress-resistant cells was detected (Fig. 6E). As expected based on the results presented above, mTORC1 activation via NV-5138 administration also increased the percentage of apoptotic cells in stressed resistant cells. Moreover, in line with the data in Fig. 3B, and in accord with our prior publication (11), Hsp70 inhibition on its own induced apoptosis in stress-sensitive cells, while the treatment was ineffective in stress-resistant cells (Fig. 6E, CTRL, +MAL3-101). Thus, mTORC1 is a major contributor to the death of stress-resistant breast cancer cells faced with a proteostasis imbalance.

Finally, given the central role of arginine as an mTORC1 activator, we monitored p-p70S6K accumulation when arginine was added to media in the presence or absence of the Hsp70 inhibitor (Fig. 6F). As expected, p-p70S6K was present to a higher extent when arginine was added to the media in stress-sensitive and resistant cells (Fig. 6C-F). As seen when mTORC1 was activated by NV-5138 (see above), a minor but statistically insignificant reduction in p-p70S6K was detected when MAL3-101 was added together with arginine, conditions under which both cell lines undergo apoptosis (Fig. 3A). Overall, these experiments confirm that mTORC1 activation (i.e., via arginine supplementation) together with ISR induction also kills cancer cells when the proteostasis pathway is imbalanced.

Discussion

All tumor cells experience proteotoxic stress due to their increased mutation rates, aneuploidy, abnormal growth, and the harsh environment (i.e., low nutrients and chemotherapeutic drug treatments) in which they can thrive. Indeed, many cancers cells avoid chemotherapy-mediated cell death, such as after treatment with DNA damaging drugs (via ISR and autophagy induction), suggesting that the inhibition of these pathways will improve chemotherapeutic efficacy (77-80). Proteotoxic stress also dysregulates nutrient balance (i.e., amino acids), and a reduction of many amino acids was reported to activate the ISR kinase, GCN2, and autophagy, as well as to repress mTORC1 signaling, thereby balancing the protein load in tumor cells and supporting tumor survival and metastasis (20, 23, 24, 43, 81). Therefore, amino acid modulation represents an increasingly desirable approach to increase cancer cell vulnerability to chemotherapy (56, 82-84).

Previously, we demonstrated that cancer cells regulate proteostasis via the ISR when challenged with MAL3-101, a site-specific allosteric inhibitor of Hsp70-mediated proteostasis (11, 36). Specifically, we found that GCN2 and autophagy prevented cell death in resistant breast lines when proteostasis was compromised (11). By using established TNBC cancer cell lines, we now show that amino acid metabolism and mTORC1 signaling impinge upon the ISR/autophagy network in these cells. We also report here that Hsp70 inhibition results in the accumulation of free amino acids in stress-sensitive but not in stress-resistant cells, strongly suggesting that proteostasis imbalance reduces the levels of select amino acids in resistant cells, which then favors GCN2 activation and autophagy. This prevents death after challenge with a chemical proteotoxic stressor. In line with our model, GCN2 induction was proposed to upregulate the levels of a lysosomal arginine-lysine transporter to increase amino acid recycling via autophagy when amino acids are depleted (85). Thus, the stress-resistant cancer cells attempt to ameliorate stress by rewiring protein degradation (autophagy), as well as ISR components, to survive and proliferate.

Our study shows that apoptosis can still be induced when resistant TNBC cells fail to reconfigure key components in the proteostasis network. Most notably, the NEAA arginine was elevated in stressed compared to MAL3-101-sensitive control cells, but not in stress-resistant cells; yet, addition of NEAAs or simply arginine to the medium of resistant cells exposed to proteotoxic stress prevented autophagy induction and resulted in cell death. While several strategies to deprive cancer cells of amino acids have been investigated (56, 86, 87), our results suggest that NEAAs—and in particular, arginine—supplementation

represents a unique strategy to enhance proteostasis collapse in TNBC cells. In line with our findings, arginine depletion induces autophagy as a cytoprotective response to proteotoxic stress in human T lymphocytes (88). Further supporting the importance of NEAA supplementation, we show that exposure of stress-sensitive cells to MAL3-101 in media deprived of amino acids reduced cancer cell death and boosted autophagy. The role of the ISR effector CHOP in breast cancer cell survival upon proteotoxic stress will need further investigation to dissect its role in favoring survival versus death. In fact, the dual nature of this protein has been reported to yield controversial results, depending on the cellular context, when using gene knock down approaches (89, 90). Given that TNBC is especially invasive, has a higher recurrence rate, and patients have limited treatment options, our study may ultimately yield new strategies to increase treatment efficacy in TNBC.

Our data also hint at the complexity of how cellular amino acids sustain cancer cells. Some cancer cells have altered arginine metabolism since this amino acid is involved in both protein synthesis and the biosynthesis of nitric oxide, polyamines, nucleosides, proline, and glutamine, in preserving ER and mitochondrial homeostasis (85, 91), as well as in mTORC1 activation; arginine has also been implicated in the T cell-mediated immune response in TNBC (54, 92-94). Further investigations will dissect the links between arginine-dependent gene expression, the ISR, and mTORC1 in TNBC.

In addition to its well documented role as a tumor promoter, mTORC1 exhibits tumor suppressive features in nutrient-poor environments (95). As mentioned above, amino acid deprivation activates GCN2 and represses mTORC1. Our experiments in MAL3-101 treated cells suggest that reduced mTORC1 activation maintains proteostasis when cancer cells are stressed, potentially by dampening mRNA translation and boosting autophagy. In fact, we show that breast cancer cell viability is reduced after mTORC1 activation via NV-5138 treatment in the presence of proteotoxic stress. It is noteworthy that we demonstrated that arginine supplementation induces mTORC1 and sustains ISR activation in the presence of MAL3-101, leading to breast cancer cell death. These results strongly suggest that proteotoxic stress-induced apoptosis is mediated by aberrant activation of mTORC1 when amino acid availability is limiting, at least in stress-resistant cells. Recent work also suggested that amino acid limitation as well as tRNA synthetase deficiency affect elongation during mRNA translation, independent of mTORC1 inhibition and GCN2-ISR activation (96-98). Moreover, ribosome pausing via amino acid deprivation might activate GCN2 and inhibit mTORC1 (45, 97). Therefore, we cannot exclude the possibility that arginine addition paired with mTORC1 activation might dysregulate protein synthesis, ultimately leading to cell death. Additional studies will delineate how arginine contributes to mTORC1 activation and mRNA translation in cancer cells challenged with a proteotoxic stressor.

In summary, our work highlights the interplay between amino acid metabolism, ISR, autophagy and mTORC1 in TNBC resistance to proteotoxic stress. Our work also supports ongoing efforts to modulate amino acid abundance and GCN2 in cancer (20, 92, 93, 99, 100). Because we showed that MAL3-101 increases the misfolded protein pool, we suggest that resistant cancer cells evolved to rely on GCN2-induced autophagy to reduce this pool of toxic, aggregation-prone proteins. At the same time, reduced amino acid abundance suppresses mTORC1, dampening protein synthesis and increasing lysosomal biogenesis

and autophagy, further supporting adaptation in stressed cancer cells. On the contrary, in stress-sensitive cells, Hsp70 inhibition activates PERK and increases free amino acids, which favors mTORC1 activation, leading to cancer cell death. Additional investigations and chemical optimization of autophagy and chaperone inhibitors, such as MAL3-101, may ultimately yield effective combination treatments for breast cancer, and in particular, TNBC.

Supplementary Material

Refer to Web version on PubMed Central for supplementary material.

Acknowledgments

We thank Drs. Desirae L. Crocker and Mary Liang for the preparation of MAL3-101. We acknowledge the Department of Biological Sciences Microscopy and Imaging core (RRID:SCR_022084) for Flow Cytometry and live confocal imaging. This work was supported by grants GM131732 to J.L.B. and S10OD023402 to S.G.W. from the National Institutes of Health, and by a UPMC Hillman Cancer Center Developmental Funding program award to J.L.B.

References

1. Kovalski JR, Kuzuoglu-Ozturk D, and Ruggero D, Protein synthesis control in cancer: selectivity and therapeutic targeting. EMBO J, 2022. 41(8): p. e109823. [PubMed: 35315941]
2. McConkey DJ, The integrated stress response and proteotoxicity in cancer therapy. Biochem Biophys Res Commun, 2017. 482(3): p. 450–453. [PubMed: 28212730]
3. Costa-Mattioli M and Walter P, The integrated stress response: From mechanism to disease. Science, 2020. 368(6489).
4. Koromilas AE, Roles of the translation initiation factor eIF2alpha serine 51 phosphorylation in cancer formation and treatment. Biochim Biophys Acta, 2015. 1849(7): p. 871–80. [PubMed: 25497381]
5. Wek RC, Role of eIF2alpha Kinases in Translational Control and Adaptation to Cellular Stress. Cold Spring Harb Perspect Biol, 2018. 10(7).
6. Wortel IMN, et al. , Surviving Stress: Modulation of ATF4-Mediated Stress Responses in Normal and Malignant Cells. Trends Endocrinol Metab, 2017. 28(11): p. 794–806. [PubMed: 28797581]
7. Ye J, et al. , The GCN2-ATF4 pathway is critical for tumour cell survival and proliferation in response to nutrient deprivation. EMBO J, 2010. 29(12): p. 2082–96. [PubMed: 20473272]
8. Walter P and Ron D, The unfolded protein response: from stress pathway to homeostatic regulation. Science, 2011. 334(6059): p. 1081–6. [PubMed: 22116877]
9. Tian X, et al. , Targeting the Integrated Stress Response in Cancer Therapy. Front Pharmacol, 2021. 12: p. 747837. [PubMed: 34630117]
10. Grandjean JMD and Wiseman RL, Small molecule strategies to harness the unfolded protein response: where do we go from here? J Biol Chem, 2020. 295(46): p. 15692–15711. [PubMed: 32887796]
11. Sannino S, et al. , Unique integrated stress response sensors regulate cancer cell susceptibility when Hsp70 activity is compromised. Elife, 2021. 10.
12. Dikic I and Elazar Z, Mechanism and medical implications of mammalian autophagy. Nat Rev Mol Cell Biol, 2018.
13. Kocaturk NM and Gozuacik D, Crosstalk Between Mammalian Autophagy and the Ubiquitin-Proteasome System. Front Cell Dev Biol, 2018. 6: p. 128. [PubMed: 30333975]
14. Milani M, et al. , The role of ATF4 stabilization and autophagy in resistance of breast cancer cells treated with Bortezomib. Cancer Res, 2009. 69(10): p. 4415–23. [PubMed: 19417138]
15. Miller DR and Thorburn A, Autophagy and organelle homeostasis in cancer. Dev Cell, 2021. 56(7): p. 906–918. [PubMed: 33689692]

16. B'Chir W, et al. , The eIF2alpha/ATF4 pathway is essential for stress-induced autophagy gene expression. Nucleic Acids Res, 2013. 41(16): p. 7683–99. [PubMed: 23804767]
17. Mizushima N, et al. , Autophagy fights disease through cellular self-digestion. Nature, 2008. 451(7182): p. 1069–75. [PubMed: 18305538]
18. Amaravadi RK, Kimmelman AC, and Debnath J, Targeting Autophagy in Cancer: Recent Advances and Future Directions. Cancer Discov, 2019. 9(9): p. 1167–1181. [PubMed: 31434711]
19. White J, Defining Target Volumes in Breast Cancer Radiation Therapy for the Future: Back to Basics. Int J Radiat Oncol Biol Phys, 2015. 93(2): p. 277–80. [PubMed: 26383677]
20. Tsun ZY and Possemato R, Amino acid management in cancer. Semin Cell Dev Biol, 2015. 43: p. 22–32. [PubMed: 26277542]
21. Baird TD and Wek RC, Eukaryotic initiation factor 2 phosphorylation and translational control in metabolism. Adv Nutr, 2012. 3(3): p. 307–21. [PubMed: 22585904]
22. Pavlova NN and Thompson CB, The Emerging Hallmarks of Cancer Metabolism. Cell Metab, 2016. 23(1): p. 27–47. [PubMed: 26771115]
23. Wei Z, et al. , Metabolism of Amino Acids in Cancer. Frontiers in Cell and Developmental Biology, 2021. 8.
24. Saxton RA and Sabatini DM, mTOR Signaling in Growth, Metabolism, and Disease. Cell, 2017. 169(2): p. 361–371.
25. Wolfson RL and Sabatini DM, The Dawn of the Age of Amino Acid Sensors for the mTORC1 Pathway. Cell Metab, 2017. 26(2): p. 301–309. [PubMed: 28768171]
26. Efeyan A, et al. , Regulation of mTORC1 by the Rag GTPases is necessary for neonatal autophagy and survival. Nature, 2013. 493(7434): p. 679–83. [PubMed: 23263183]
27. Nakamura A, et al. , Inhibition of GCN2 sensitizes ASNS-low cancer cells to asparaginase by disrupting the amino acid response. Proc Natl Acad Sci U S A, 2018. 115(33): p. E7776–E7785. [PubMed: 30061420]
28. Sannino S and Brodsky JL, Targeting protein quality control pathways in breast cancer. BMC Biol, 2017. 15(1): p. 109. [PubMed: 29145850]
29. Garrido C, et al. , Heat shock proteins 27 and 70: anti-apoptotic proteins with tumorigenic properties. Cell Cycle, 2006. 5(22): p. 2592–601. [PubMed: 17106261]
30. Mosser DD and Morimoto RI, Molecular chaperones and the stress of oncogenesis. Oncogene, 2004. 23(16): p. 2907–18. [PubMed: 15077153]
31. Brodsky JL and Chiosis G, Hsp70 molecular chaperones: emerging roles in human disease and identification of small molecule modulators. Curr Top Med Chem, 2006. 6(11): p. 1215–25. [PubMed: 16842158]
32. Shao H, et al. , A campaign targeting a conserved Hsp70 binding site uncovers how subcellular localization is linked to distinct biological activities. Cell Chem Biol, 2022. 29(8): p. 1303–1316 e3. [PubMed: 35830852]
33. Powers MV, et al. , Targeting HSP70: the second potentially druggable heat shock protein and molecular chaperone? Cell Cycle, 2010. 9(8): p. 1542–50. [PubMed: 20372081]
34. Fewell SW, Day BW, and Brodsky JL, Identification of an inhibitor of hsc70-mediated protein translocation and ATP hydrolysis. J Biol Chem, 2001. 276(2): p. 910–4. [PubMed: 11036084]
35. Wisen S, et al. , Binding of a small molecule at a protein-protein interface regulates the chaperone activity of hsp70-hsp40. ACS Chem Biol, 2010. 5(6): p. 611–22. [PubMed: 20481474]
36. Sannino S, et al. , Compensatory increases of select proteostasis networks after Hsp70 inhibition in cancer cells. J Cell Sci, 2018. 131(17).
37. Sabnis AJ, et al. , Combined chemical-genetic approach identifies cytosolic HSP70 dependence in rhabdomyosarcoma. Proc Natl Acad Sci U S A, 2016. 113(32): p. 9015–20. [PubMed: 27450084]
38. Fewell SW, et al. , Small molecule modulators of endogenous and co-chaperone-stimulated Hsp70 ATPase activity. J Biol Chem, 2004. 279(49): p. 51131–40. [PubMed: 15448148]
39. Earnshaw WC, Martins LM, and Kaufmann SH, Mammalian caspases: structure, activation, substrates, and functions during apoptosis. Annu Rev Biochem, 1999. 68: p. 383–424. [PubMed: 10872455]

40. Lee AV and Davidson NE, Breast cancer in 2013: Genomics, drug approval, and optimal treatment duration. Nat Rev Clin Oncol, 2014. 11(2): p. 71–2. [PubMed: 24419301]
41. Waks AG and Winer EP, Breast Cancer Treatment: A Review. JAMA, 2019. 321(3): p. 288–300. [PubMed: 30667505]
42. Yin L, et al. , Triple-negative breast cancer molecular subtyping and treatment progress. Breast Cancer Res, 2020. 22(1): p. 61. [PubMed: 32517735]
43. Vettore L, Westbrook RL, and Tennant DA, New aspects of amino acid metabolism in cancer. Br J Cancer, 2020. 122(2): p. 150–156. [PubMed: 31819187]
44. Meijer AJ, et al. , Regulation of autophagy by amino acids and MTOR-dependent signal transduction. Amino Acids, 2015. 47(10): p. 2037–63. [PubMed: 24880909]
45. Harding HP, et al. , The ribosomal P-stalk couples amino acid starvation to GCN2 activation in mammalian cells. Elife, 2019. 8.
46. Battu S, et al. , Amino Acid Sensing via General Control Nonderepressible-2 Kinase and Immunological Programming. Front Immunol, 2017. 8: p. 1719. [PubMed: 29321774]
47. Antonucci L, et al. , Basal autophagy maintains pancreatic acinar cell homeostasis and protein synthesis and prevents ER stress. Proc Natl Acad Sci U S A, 2015. 112(45): p. E6166–74. [PubMed: 26512112]
48. Fitzwalter BE, et al. , Autophagy Inhibition Mediates Apoptosis Sensitization in Cancer Therapy by Relieving FOXO3a Turnover. Dev Cell, 2018. 44(5): p. 555–565 e3. [PubMed: 29533771]
49. Chen Y and Zhou X, Research progress of mTOR inhibitors. Eur J Med Chem, 2020. 208: p. 112820. [PubMed: 32966896]
50. Manifava M, et al. , Dynamics of mTORC1 activation in response to amino acids. Elife, 2016. 5.
51. Zoncu R, et al. , mTORC1 senses lysosomal amino acids through an inside-out mechanism that requires the vacuolar H(+)-ATPase. Science, 2011. 334(6056): p. 678–83. [PubMed: 22053050]
52. Jia JJ, et al. , mTORC1 promotes TOP mRNA translation through site-specific phosphorylation of LARP1. Nucleic Acids Res, 2021. 49(6): p. 3461–3489. [PubMed: 33398329]
53. Dent R, et al. , Triple-negative breast cancer: clinical features and patterns of recurrence. Clin Cancer Res, 2007. 13(15 Pt 1): p. 4429–34. [PubMed: 17671126]
54. Saxton RA, et al. , Mechanism of arginine sensing by CASTOR1 upstream of mTORC1. Nature, 2016. 536(7615): p. 229–33. [PubMed: 27487210]
55. Carroll B, et al. , Control of TSC2-Rheb signaling axis by arginine regulates mTORC1 activity. Elife, 2016. 5.
56. Kanarek N, Petrova B, and Sabatini DM, Dietary modifications for enhanced cancer therapy. Nature, 2020. 579(7800): p. 507–517. [PubMed: 32214253]
57. Shen JZ, Wu G, and Guo S, Amino Acids in Autophagy: Regulation and Function. Adv Exp Med Biol, 2021. 1332: p. 51–66. [PubMed: 34251638]
58. Kamata S, et al. , Dietary deprivation of each essential amino acid induces differential systemic adaptive responses in mice. Mol Nutr Food Res, 2014. 58(6): p. 1309–21. [PubMed: 24668850]
59. Mizushima N, The exponential growth of autophagy-related research: from the humble yeast to the Nobel Prize. FEBS Lett, 2017. 591(5): p. 681–689. [PubMed: 28186333]
60. Towers CG, Wodetzki D, and Thorburn A, Autophagy and cancer: Modulation of cell death pathways and cancer cell adaptations. J Cell Biol, 2020. 219(1).
61. Poillet-Perez L, Sarry JE, and Joffre C, Autophagy is a major metabolic regulator involved in cancer therapy resistance. Cell Rep, 2021. 36(7): p. 109528. [PubMed: 34407408]
62. Mizushima N and Klionsky DJ, Protein turnover via autophagy: implications for metabolism. Annu Rev Nutr, 2007. 27: p. 19–40. [PubMed: 17311494]
63. Kimura S, Noda T, and Yoshimori T, Dissection of the autophagosome maturation process by a novel reporter protein, tandem fluorescent-tagged LC3. Autophagy, 2007. 3(5): p. 452–60. [PubMed: 17534139]
64. Su N and Kilberg MS, C/EBP homology protein (CHOP) interacts with activating transcription factor 4 (ATF4) and negatively regulates the stress-dependent induction of the asparagine synthetase gene. J Biol Chem, 2008. 283(50): p. 35106–17. [PubMed: 18940792]

65. B'Chir W, et al. , Dual role for CHOP in the crosstalk between autophagy and apoptosis to determine cell fate in response to amino acid deprivation. Cell Signal, 2014. 26(7): p. 1385–91. [PubMed: 24657471]
66. Axten JM, et al. , Discovery of 7-methyl-5-(1-{[3-(trifluoromethyl)phenyl]acetyl}−2,3-dihydro-1H-indol-5-yl)-7H-p yrrolo[2,3-d]pyrimidin-4-amine (GSK2606414), a potent and selective first-in-class inhibitor of protein kinase R (PKR)-like endoplasmic reticulum kinase (PERK). J Med Chem, 2012. 55(16): p. 7193–207. [PubMed: 22827572]
67. Byles V, et al. , Hepatic mTORC1 signaling activates ATF4 as part of its metabolic response to feeding and insulin. Mol Metab, 2021. 53: p. 101309. [PubMed: 34303878]
68. Munoz-Pinedo C and Lopez-Rivas A, A role for caspase-8 and TRAIL-R2/DR5 in ER-stress-induced apoptosis. Cell Death Differ, 2018. 25(1): p. 226. [PubMed: 28984868]
69. Lu M, et al. , Opposing unfolded-protein-response signals converge on death receptor 5 to control apoptosis. Science, 2014. 345(6192): p. 98–101. [PubMed: 24994655]
70. Lindner P, et al. , Cell death induced by the ER stressor thapsigargin involves death receptor 5, a non-autophagic function of MAP1LC3B, and distinct contributions from unfolded protein response components. Cell Commun Signal, 2020. 18(1): p. 12. [PubMed: 31987044]
71. Dufour F, et al. , TRAIL receptor gene editing unveils TRAIL-R1 as a master player of apoptosis induced by TRAIL and ER stress. Oncotarget, 2017. 8(6): p. 9974–9985. [PubMed: 28039489]
72. Hu P, et al. , Autocrine tumor necrosis factor alpha links endoplasmic reticulum stress to the membrane death receptor pathway through IRE1alpha-mediated NF-kappaB activation and down-regulation of TRAF2 expression. Mol Cell Biol, 2006. 26(8): p. 3071–84. [PubMed: 16581782]
73. Timmins JM, et al. , Calcium/calmodulin-dependent protein kinase II links ER stress with Fas and mitochondrial apoptosis pathways. J Clin Invest, 2009. 119(10): p. 2925–41. [PubMed: 19741297]
74. Laplante M and Sabatini DM, mTOR Signaling. Cold Spring Harb Perspect Biol, 2012. 4(2).
75. Rabinowitz JD and White E, Autophagy and metabolism. Science, 2010. 330(6009): p. 1344–8. [PubMed: 21127245]
76. Kato T, et al. , Sestrin modulator NV-5138 produces rapid antidepressant effects via direct mTORC1 activation. J Clin Invest, 2019. 129(6): p. 2542–2554. [PubMed: 30990795]
77. Guo JY, et al. , Autophagy provides metabolic substrates to maintain energy charge and nucleotide pools in Ras-driven lung cancer cells. Genes Dev, 2016. 30(15): p. 1704–17. [PubMed: 27516533]
78. Yang A and Kimmelman AC, Inhibition of autophagy attenuates pancreatic cancer growth independent of TP53/TRP53 status. Autophagy, 2014. 10(9): p. 1683–4. [PubMed: 25046107]
79. Nedeljkovic M and Damjanovic A, Mechanisms of Chemotherapy Resistance in Triple-Negative Breast Cancer-How We Can Rise to the Challenge. Cells, 2019. 8(9).
80. Chen L, et al. , EIF2A promotes cell survival during paclitaxel treatment in vitro and in vivo. J Cell Mol Med, 2019. 23(9): p. 6060–6071. [PubMed: 31211507]
81. Nofal M, et al. , GCN2 adapts protein synthesis to scavenging-dependent growth. Cell Syst, 2022. 13(2): p. 158–172 e9. [PubMed: 34706266]
82. Geiger R, et al. , L-Arginine Modulates T Cell Metabolism and Enhances Survival and Anti-tumor Activity. Cell, 2016. 167(3): p. 829–842 e13. [PubMed: 27745970]
83. Anderson PM and Lalla RV, Glutamine for Amelioration of Radiation and Chemotherapy Associated Mucositis during Cancer Therapy. Nutrients, 2020. 12(6).
84. Wang H, et al. , High dose isoleucine stabilizes nuclear PTEN to suppress the proliferation of lung cancer. Discov Oncol, 2023. 14(1): p. 25. [PubMed: 36820928]
85. Higuchi-Sanabria R, et al. , Lysosomal recycling of amino acids affects ER quality control. Sci Adv, 2020. 6(26): p. eaaz9805. [PubMed: 32637599]
86. Du T and Han J, Arginine Metabolism and Its Potential in Treatment of Colorectal Cancer. Front Cell Dev Biol, 2021. 9: p. 658861. [PubMed: 34095122]
87. Pathria G and Ronai ZA, Harnessing the Co-vulnerabilities of Amino Acid-Restricted Cancers. Cell Metab, 2021. 33(1): p. 9–20. [PubMed: 33406406]
88. Garcia-Navas R, Munder M, and Mollinedo F, Depletion of L-arginine induces autophagy as a cytoprotective response to endoplasmic reticulum stress in human T lymphocytes. Autophagy, 2012. 8(11): p. 1557–76. [PubMed: 22874569]

89. Zhou AX, et al. , C/EBP-Homologous Protein (CHOP) in Vascular Smooth Muscle Cells Regulates Their Proliferation in Aortic Explants and Atherosclerotic Lesions. Circ Res, 2015. 116(11): p. 1736–43. [PubMed: 25872946]

90. Fan L, et al. , Melatonin reverses tunicamycin-induced endoplasmic reticulum stress in human hepatocellular carcinoma cells and improves cytotoxic response to doxorubicin by increasing CHOP and decreasing survivin. J Pineal Res, 2013. 55(2): p. 184–94. [PubMed: 23711089]

91. Barros CDS, et al. , L-Arginine Reduces Nitro-Oxidative Stress in Cultured Cells with Mitochondrial Deficiency. Nutrients, 2021. 13(2).

92. Cordova RA, et al. , GCN2 eIF2 kinase promotes prostate cancer by maintaining amino acid homeostasis. Elife, 2022. 11.

93. Cao Y, et al. , L-Arginine supplementation inhibits the growth of breast cancer by enhancing innate and adaptive immune responses mediated by suppression of MDSCs in vivo. BMC Cancer, 2016. 16: p. 343. [PubMed: 27246354]

94. Cao Y, et al. , l-arginine and docetaxel synergistically enhance anti-tumor immunity by modifying the immune status of tumor-bearing mice. Int Immunopharmacol, 2016. 35: p. 7–14. [PubMed: 27003114]

95. Villar VH, et al. , mTORC1 inhibition in cancer cells protects from glutaminolysis-mediated apoptosis during nutrient limitation. Nat Commun, 2017. 8: p. 14124. [PubMed: 28112156]

96. Pitera AP, et al. , Cellular responses to halofuginone reveal a vulnerability of the GCN2 branch of the integrated stress response. EMBO J, 2022. 41(11): p. e109985. [PubMed: 35466425]

97. Darnell AM, Subramaniam AR, and O'Shea EK, Translational Control through Differential Ribosome Pausing during Amino Acid Limitation in Mammalian Cells. Mol Cell, 2018. 71(2): p. 229–243 e11. [PubMed: 30029003]

98. Goodarzi H, et al. , Modulated Expression of Specific tRNAs Drives Gene Expression and Cancer Progression. Cell, 2016. 165(6): p. 1416–1427. [PubMed: 27259150]

99. Barbosa-Tessmann IP, et al. , Activation of the human asparagine synthetase gene by the amino acid response and the endoplasmic reticulum stress response pathways occurs by common genomic elements. J Biol Chem, 2000. 275(35): p. 26976–85. [PubMed: 10856289]

100. Misra J, et al. , Discordant regulation of eIF2 kinase GCN2 and mTORC1 during nutrient stress. Nucleic Acids Res, 2021. 49(10): p. 5726–5742. [PubMed: 34023907]

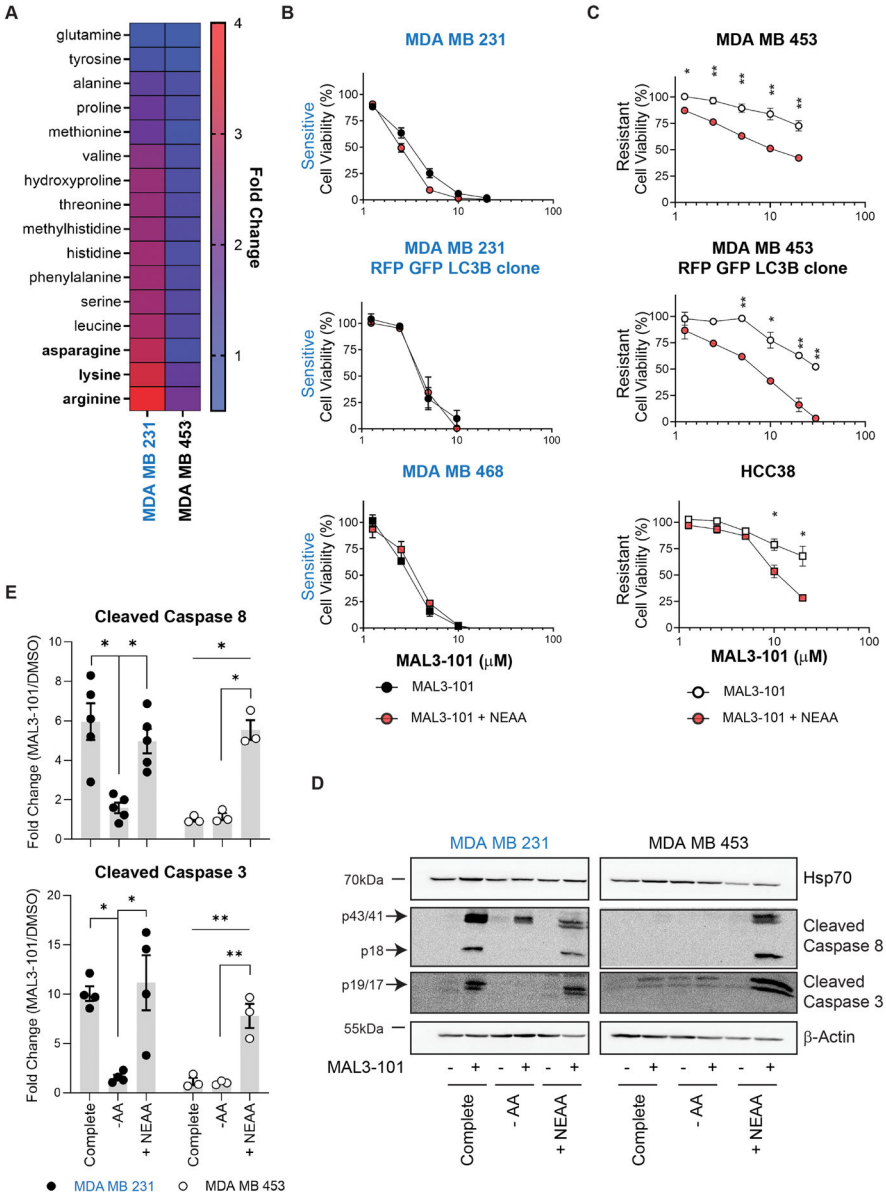

Figure 1. Non-essential amino acids trigger apoptosis in stress-resistant breast cancer cells after exposure to a proteostasis poison.

A, Stress-sensitive (MDA MB 231) and resistant (MDA MB 453) cells were treated with 5 μM MAL3-101 or vehicle control for 24 h, followed by lysis and amino acids analysis. The heatmap represents the mean fold change (treated/vehicle) of the analyzed amino acids from 4 replicates from 2 independent experiments. **B-C,** Stress-sensitive and -resistant cells (indicated with blue and black text, respectively) were treated with increasing doses of MAL3-101 in the presence or absence of NEAAs. Cell viability was measured after 72 h, and data represent the means of 3 independent experiments, ± SEM. *$p < 0.05$; **$p < 0.005$. **D,** Stress-sensitive (in blue) and resistant (in black) cells were treated with 20 μM MAL3-101 for 5 h in complete media, upon NEAA supplementation, or when amino acids were deprived. Samples were analyzed for cleaved caspase-3 and caspase-8 expression. β-actin was used as loading control. **E,** The corresponding fold change of the indicated

apoptotic markers relative to the DMSO control are plotted ± SEM (n=4 cleaved caspase-3 and n=5 cleaved caspase-8 for MDA MB 231 cells, n=3 cleaved caspase-3 and caspase =−8 for MDA MB 453 cells) *$p < 0.05$; **$p < 0.005$.

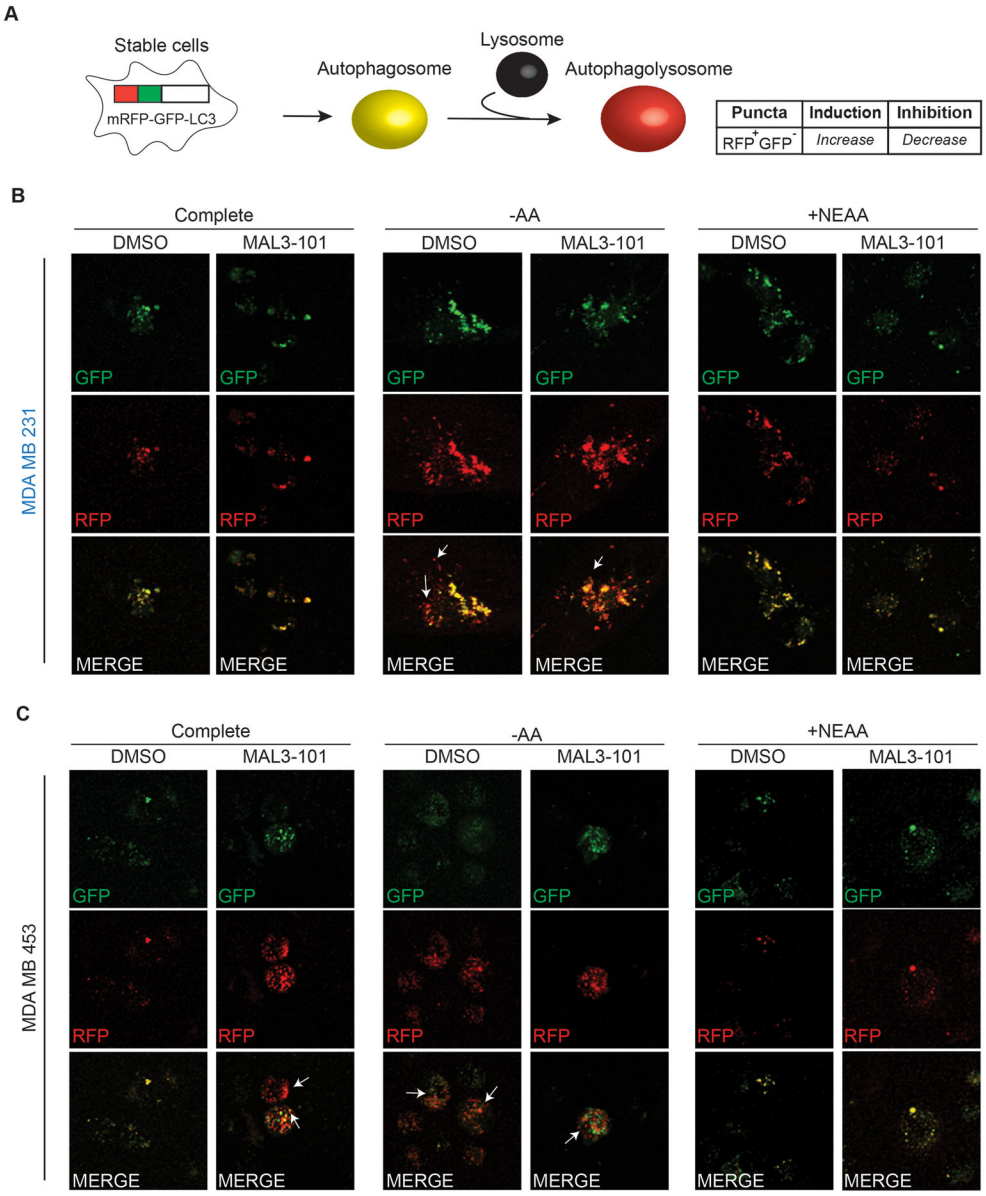

Figure 2. Modulating amino acid abundance alters autophagic flux in the presence of MAL3-101, an Hsp70 inhibitor.

A, Autophagosomes (RFP^+GFP^+) and autophagolysosomes (RFP^+GFP^-) are distinguished as yellow and red puncta, respectively. Accumulation of RFP^+GFP^- indicates increased autophagy flux, while visualization of yellow puncta is reflective of autophagy inhibition. **B-C,** Confocal images of stress-sensitive (MDA MB 231, in blue) and resistant (MDA MB 453, in black) cells treated with MAL3-101 for 5 h in different conditions. White arrows indicated examples of RFP^+GFP^- puncta (autophagolysosomes). Minor changes in cell morphology were detected when MDA MB 453 cells were exposed to MAL3-101 in complete and amino acid deprived media. These changes do not correspond to cell death data (as shown in Figure 1 and 3).

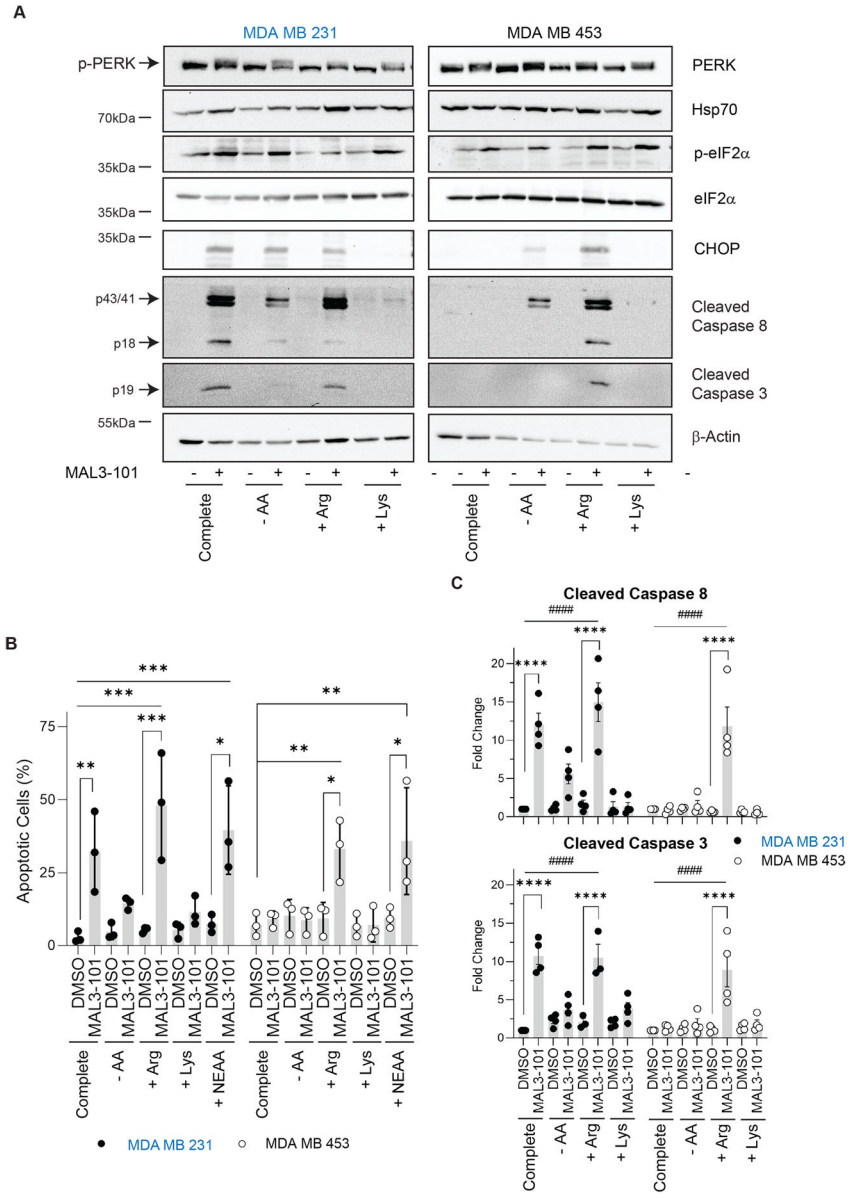

Figure 3. Arginine is sufficient to trigger apoptosis in stress-resistant breast cancer cells.

A, Stress-sensitive (in blue) and -resistant (in black) cells were treated with 20 μM MAL3-101 or DMSO for 5 h in the indicated media, and lysates were prepared for immunoblot analysis. β-actin was used as loading control. **B,** Cells were treated as in panel A before annexin-V and PI staining. The sum of annexin-V and annexin-V and PI double positive cells is represented in the graph and indicated as the percentage of apoptotic cells. Stress-sensitive cells (in blue) are indicated with closed symbols and resistant cells (in black) by open circles. The means of 3 independent experiments, ± SD, are indicated. *p < 0.05; **p < 0.005; *** p<0.0005. **C,** The corresponding fold increase of cleaved caspase-3 and cleaved caspase-8 in stress-sensitive (closed symbols) and resistant (open symbols) cells was measured after incubation in complete media or media lacking added amino acids (-AA), or containing arginine (+Arg) or lysine (+Lys) in the presence or absence of

MAL3-101. The fold change is shown relative to DMSO (control), ± SEM (n=4). Asterisks (*) indicate statistically significant comparisons between DMSO and MAL3-101 treatments for each media condition, while # represents statistically significant comparisons between DMSO complete and the other conditions indicated for each line. ****/#### $p<0.0001$.

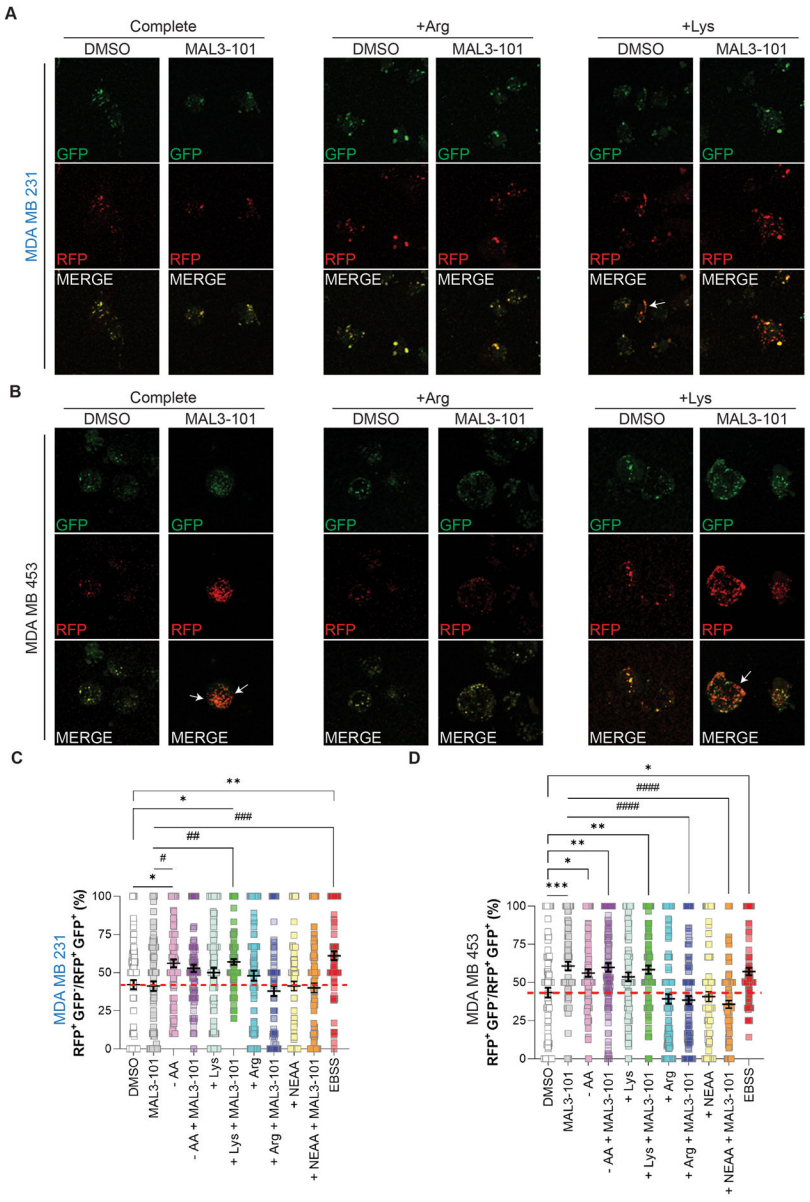

Figure 4. Arginine blocks proteotoxic stress-dependent autophagy in resistant cells.

A-B, Confocal images of stress-sensitive (MDA MB 231, in blue) and -resistant (MDA MB 453, in black) cells treated with MAL3-101 for 5 h in complete media or in media supplemented only with arginine (+Arg) or lysine (+Lys). White arrows indicated examples of RFP^+GFP^- puncta (autophagolysosomes). **C-D,** The percent of RFP^+GFP^- (autophagolysosome) or RFP^+GFP^+ (autophagosome) puncta per cell is reported for stress-sensitive (**C**) and resistant (**D**) lines, treated as indicated in Figure 2, ± SEM (n≥90). The calculated ratios are indicative of the percentage of autophagosomes (RFP^+GFP^+) that mature into autophagolysosomes (RFP^+GFP^-), which are degradation active autophagic vesicles. Statistically significant differences between DMSO and cells incubated in starvation media (EBSS, positive control) or treated with media containing different amino acid levels in the presence or absence of MAL3-101 are indicated by black asterisks,

while # represents statistically significant comparisons between MAL3-101 complete and the other conditions indicated for each line. $^{*/\#}p < 0.05$; $^{**/\#\#}p < 0.005$; $^{***/\#\#\#}p<0.0005$; $^{****/\#\#\#\#}p<0.0001$.

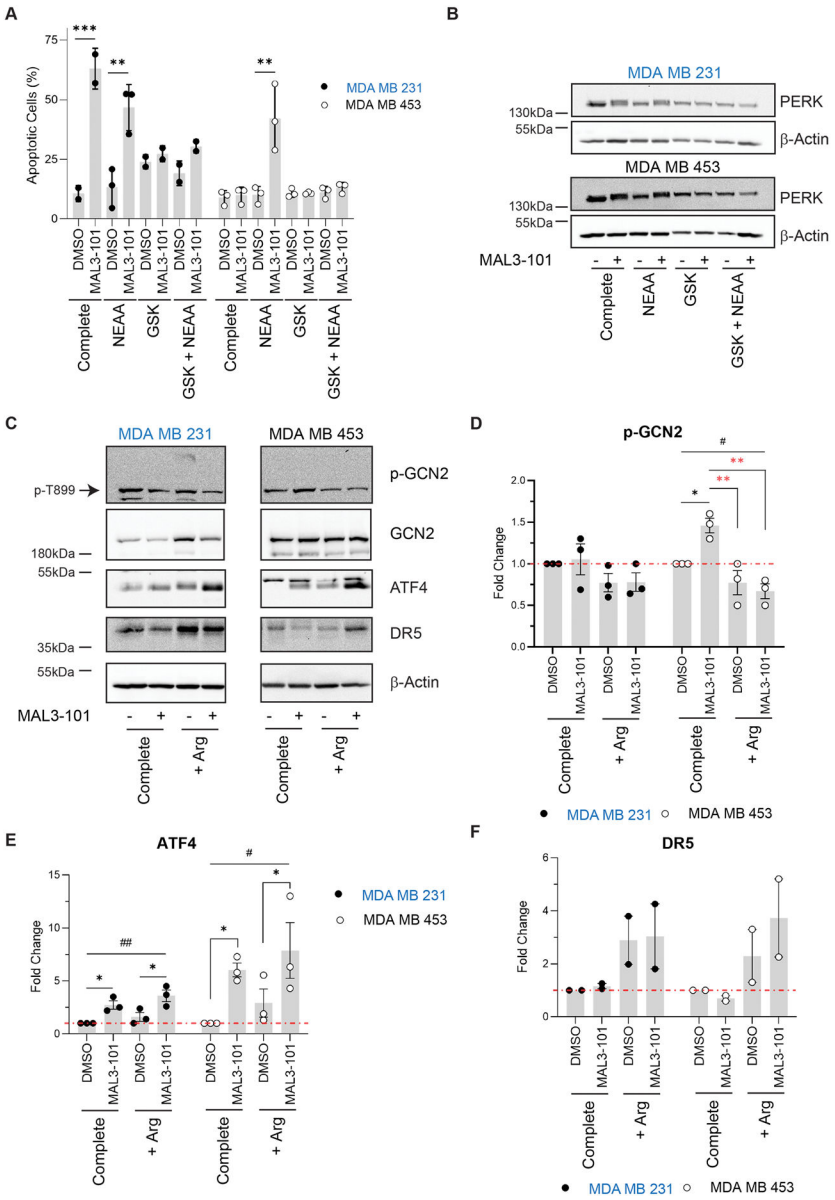

Figure 5. The role of the ISR when amino acid abundance is altered and the proteostasis pathway collapses.

A, E, Cells were treated with 20 μM MAL3-101 or DMSO for 6 h after which PERK activity was inhibited (GSK) or not in complete or NEAA supplemented media before annexin-V and PI staining were performed. The percent of apoptotic cells is represented in the graph ± SD. Stress-sensitive cells (in blue) are indicated with closed symbols and resistant cells (in black) with open circles (n=2 for MDA MB 231 cells and n=3 for MDA MB 453 cells). Asterisks (*) represent the statistical significance between MAL3-101 treated and DMSO control in all the indicated conditions. *p < 0.05; **p < 0.005; ***p<0.0005. **B,** Stress-sensitive (in blue) and resistant (in black) cells were treated with 20 μM MAL3-101 or DMSO for 5 h in the presence or absence of GSK. Lysates were immunoblotted for the indicated proteins. β-actin was used as a loading control. **C,** Stress-sensitive (in blue) and resistant (in black) cells were treated with 20 μM MAL3-101 or

DMSO for 5 h in the indicated media, and lysates were prepared for immunoblot analysis. β-actin was used as loading control. **D-F,** The corresponding fold increase of p-GCN2 (**D**), ATF4 (**E**) and DR5 (**F**), in stress-sensitive (closed symbols) and resistant (open symbols) cells was measured after incubation in complete or arginine containing media (+Arg) in the presence or absence of MAL3-101. The fold change is shown relative to DMSO (control), ± SEM (n=3 for p-GCN2 and ATF4, and n=2 for DR5). Black asterisks (*) indicate statistically significant comparisons between DMSO and MAL3-101 treatments for each media condition, while # represents statistically significant comparisons between DMSO complete and the other conditions indicated for each line. Red asterisks represent statistically significant comparisons between MAL3-101 and the other conditions. $*^{/\#}p < 0.05$; $**^{/\#\#}p < 0.005$.

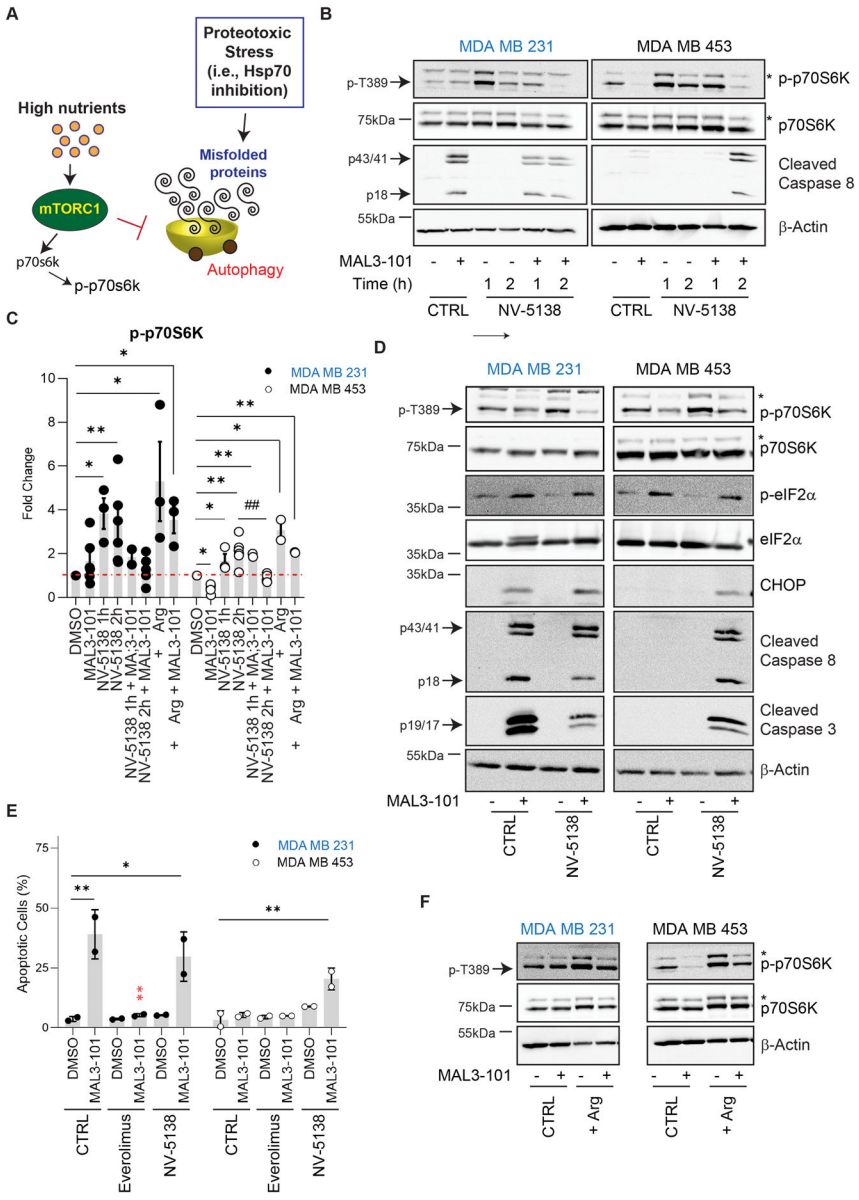

Figure 6. Discordant GCN2 and mTORC1 activation favors breast cancer cell survival upon proteotoxic stress.

A, Increased nutrient availability (i.e., amino acids) favors mTORC1 activation that in turn boosts p-p70S6K accumulation while inhibiting autophagy, thus preventing misfolded protein degradation caused by proteotoxic stress exposure (i.e., Hsp70 inhibition). **B,** Stress-sensitive (in blue) and -resistant (in black) cells were treated with 20 μM MAL3-101 or DMSO for 6 h and NV-5138 was added during the last 1 or 2 h to activate mTORC1. Lysates were immunoblotted for the indicated proteins. A non-specific band in the p-p70S6K blot is indicated with an asterisk (*), and β-actin was used as loading control. **C,** The fold increase of p-p70S6K in stress-sensitive (closed circles) and resistant (open circles) cells is shown, ± SEM as quantification of the experiments presented in panels **B**, **D,** and **F** (n=6 for MAL3-101 and NV-5138 2h, n=5 for NV-5138 2h + MAL3-101, n=3 for NV-5138 1h, +Arg and + Arg + MAL3-101, n=2 for NV-5138 1h + MAL3-101). Asterisks (*)

represent statistically significant comparisons between DMSO and conditions indicated for each line, while # indicate statistically significant comparisons between DMSO and MAL3-101 treatments for each media condition. $^{*/\#}p < 0.05$; $^{**/\#\#}p < 0.005$. **D,** Stress-sensitive (in blue) and -resistant (in black) cells were treated with 20 μM MAL3-101 or DMSO for 6 h and NV-5138 was added during the last 2 h to activate mTORC1. Lysates were immunoblotted for the indicated proteins. A non-specific band in the p-p70S6K blot is indicated with an asterisk (*), and β-actin was used as loading control. **E,** Cells were treated with 20 μM MAL3-101 or DMSO for 6 h when mTORC1 activity was inhibited (everolimus) or activated (NV-5138) or in vehicle treated conditions before annexin-V and PI staining. The percent of apoptotic cells is represented in the graph. Stress-sensitive cells (in blue) are indicated with closed symbols and resistant cells (in black) with open circles. The means of 2 independent experiments, ± SD, are indicated. Red asterisks represent the statistical significance between MAL3-101 treated CTRL and -AA MAL3-101 samples, while black asterisks indicate the statistical significance between the DMSO control, and all indicated conditions. *p < 0.05; **p < 0.005. **F,** Stress-sensitive (in blue) and resistant (in black) cells were treated with 20 μM MAL3-101 or DMSO for 6 h in the indicated media, and lysates were prepared for immunoblot analysis. β-actin was used as loading control. A non-specific band in the p-p70S6K blot is indicated with an asterisk (*).